Yield of EEG features as markers of disease severity in Amyotrophic Lateral Sclerosis: a pilot study

Notturno Francesca[1], Croce Pierpaolo[2,3 *], Ornello Raffaele[4], Sacco Simona[4], Zappasodi Filippo[2,3,5]

[1]*Unit of Neurology,'Floraspe Renzetti' Hospital, Lanciano, Italy*

[2]*Department of Neuroscience, Imaging and Clinical Sciences, University 'Gabriele d'Annunzio' of Chieti-Pescara, Chieti, Italy*

[3] *Behavioral Imaging and Neural Dynamics Center, University "Gabriele d'Annunzio" of Chieti–Pescara, Chieti, Italy*

[4]*Department of Biotechnological and Applied Clinical Sciences, University of L'Aquila, L'Aquila, Italy*

[5] *Institute for Advanced Biomedical Technologies, University "Gabriele d'Annunzio" of Chieti–Pescara, Chieti, Italy*

[*]Corresponding author:

Dr Pierpaolo Croce,

'Gabriele d'Annunzio' University of Chieti-Pescara,

via dei Vestini, 66100, Chieti, Italy

phone: +39 0861 3556943

email: pierpaolo.croce@unich.it

Yield of EEG features as markers of disease severity in Amyotrophic Lateral Sclerosis: a pilot study

Objective: To clarify the role of electroencephalography (EEG) as a promising marker of severity in amyotrophic lateral sclerosis (ALS).

We characterized the brain spatio-temporal patterns activity at rest by means of both spectral band powers and EEG microstates and correlated these features with clinical scores.

Methods: Eyes closed EEG was acquired in 15 patients with ALS and spectral band power was calculated in frequency bands, defined on the basis of individual alpha frequency (IAF): delta-theta band (1-7 Hz); low alpha (IAF–2 Hz - IAF); high alpha (IAF - IAF+2 Hz); beta (13-25 Hz). EEG microstate metrics (duration, occurrence, coverage) were also evaluated. Spectral band powers and microstate metrics were correlated with several clinical scores of disabilities and disease progression. As a control group, 15 healthy volunteers were enrolled.

Results: The beta-band power in motor/frontal regions was higher in patients with higher disease burden, negatively correlated with clinical severity scores and positively correlated with disease progression. Overall microstate duration was longer and microstate occurrence was lower in patients than in controls. Longer duration was correlated with a worse clinical status.

Conclusions: Our results showed that beta-band power and microstate metrics may be good candidates of disease severity in ALS. Increased beta and longer microstate duration in clinically worse patients suggest a possible impairment of both motor and non-motor network activities to fast modify their status. This can be interpreted as an attempt in ALS patients to compensate the disability but resulting in an ineffective and probably maladaptive behaviour.

Keywords: disease severity; beta band; EEG microstate; electrophysiological marker.

Introduction

The diagnosis of Amyotrophic Lateral Sclerosis (ALS) is based on the presence of clinical findings in conjunction with investigations to exclude "ALS-mimic" syndromes. The presence of signs of combined upper and lower motor neurons (UMN and LMN) damage, that cannot be explained by any other disease processes, together with progression, is suggestive of ALS. Different diagnostic criteria (1–3) have been developed to aid in diagnosis and in classifying patients for research studies and drug trials. Markers of disease severity and progression are interesting targets, since they may provide objective measures to be used in clinical intervention and in randomized control-trial designs, and in turn, may bring to light targets for novel therapies. Clinical trial endpoints currently involve measures, such as survival or the revised ALS functional rating scale (ALSFRS-R (4)). Such outcomes need to be monitored over long periods of time before a conclusion can be drawn, resulting in an expensive and ineffective process (5). Electrophysiological (Motor Unit Number Estimation, Motor Unit Number Index, neurophysiological indexes), as well as biochemical (oxidative stress, inflammatory indicators) and metabolic (proteomics, neurofilament proteins) biomarkers from serum and cerebral spinal fluid, have been proposed, but with different and sometimes conflicting results, requiring further investigation (5).

Magnetic resonance imaging (MRI) does not involve ionizing radiations and is a non-invasive technique. There is a large body of published work in the context of ALS, mainly focused on the UMN, with fewer studies relating to the spinal cord, muscle and peripheral nerve (6–9). Moreover, by functional MRI (fMRI) several studies evidenced resting brain network degeneration in ALS patients, originating from the motor cortex and spreading to non-motor areas (10–14), and discriminating between fast and slow progression (15).

Electroencephalography (EEG) may also be a promising technique for capturing the brain activity at rest in ALS patients. Compared with MRI or fMRI, EEG is available in most neurology centres, has a good time resolution, is easily applicable, has no contraindications and is inexpensive. Moreover, EEG features and changes can be independent of selective UMN and LMN involvement. Until now, only few EEG studies investigated resting functional changes in ALS patients and their possible correlation with clinical measures. An increased connectivity was found in ALS patients with respect to healthy controls, in broad frequency band in the frontal and parietal regions (16,17), but these changes were not related to the clinical status. However, a tendency to deviate towards a more decentralized organization, correlating with disability, was found in the topology of resting-state functional networks in beta band (18). Moreover, an increase of functional connectivity in theta band between bilateral motor areas was associated with disease progression (19). Finally, a widespread decrease of low frequency band power, as well as a decrease in beta band in sensorimotor regions, was found in ALS patients with respect to controls (20). Furthermore, in both motor and non-motor brain networks, changes in functional connectivity, correlating with structural damage and clinical scores, were described (20).

In ALS patients, non-motor areas involvement has been hypothesized (21), but their dynamics of interactions is not even clear. Nevertheless, the use of spectral EEG band powers to investigate the dynamics of brain spontaneous resting-state activity is a non-trivial task, as the signal of interest is of low amplitude and it may be difficult to characterize the underlying neural sources (22). To address this challenge, several previous studies investigated these dynamics by the sequence of EEG topographies, namely “microstates”. By microstate analysis, the whole brain activity is modelled by a

sequence of few scalp topographies, each associated with a functional brain state during the occurrence of specific neural processes (23). Microstate analysis, compared to the classical EEG resting-state analysis, does not blur by averaging the activities of different brain networks, preserving their dynamics. Different studies of EEG at rest converged in finding four topographical map templates. The temporal features of these maps have been found to be modulated by awareness or behavioural/cognitive control (24–28) and altered in brain diseases (29–31).

Considering few previous studies, with inconclusive results regarding the relation between EEG changes and clinical severity, we aimed to clarify the role of quantitative resting EEG. We investigated a possible link between spectral EEG band powers and several clinical scores of disability, as well as disease progression. Such characteristics may represent a promising electrophysiological marker of disease severity in ALS. Morevover, to our knowledge no microstate studies have been performed to assess changes of brain spatio-temporal patterns activity at rest, in ALS patients. If the microstate sequences describe the fluctuations across main states of brain networks (32), we can expect some changes of microstate typical in ALS patients. Such features may represent an attractive electrophysiological marker of involvement and progression of non-motor areas in ALS.

Materials and Methods

Patients and clinical evaluation

Fifteen patients with ALS (see Table 1 for inclusion and exclusion criteria) and 15 age- and gender-balanced healthy controls were enrolled in the study. All but two patients were taking Riluzole at the time of the study. The two patients not taking Riluzole had

stopped the drug due to side effects.

INSERT TABLE 1 HERE

The experiment was conducted with the understanding and written informed consent of each participant, according to the Code of Ethics of the World Medical Association. Participants acknowledged that they cannot be identified via the study and that their data were fully anonymized. The experimental protocol was approved by the Ethics Committee for the Districts of L'Aquila and Teramo.

Each patient underwent clinical evaluation at 2 times: after recruitment (T0) and at 3 months (T1). Clinical evaluation is summarized in Table 2.

INSERT TABLE 2 HERE

EEG recording and data analysis

At time T1, five minutes of EEG activity at rest with eyes closed was recorded by a 128 channels EEG system (Electrical Geodesic Inc, EEG System Net 300), while subject was sitting or lying. Skin/electrode impedance was measured before EEG recording and kept below 50 kΩ. EEG data were sampled at 250 Hz and processed off-line.

Data were visually checked and bad epochs were excluded by the analysis. Bad channels were replaced by spline interpolation of neighbouring channels (33). A semiautomatic Independent Component Analysis-based procedure (34,35) was applied to identify and remove cardiac and/or ocular artifacts. Scalp EEG recordings were filtered between 1 and 30 Hz (Butterworth filter of 2nd order, forward and back filtering) and referenced to the common average.

The Power Spectral Density (PSD) was estimated for each EEG channel via the Welch procedure (frequency resolution of 0.25 Hz, Hanning windowing, 60% overlap). For each EEG electrode band power values were obtained as the mean of PSD in each

frequency band. The investigated frequency bands were individually defined on the basis of Individual Alpha Frequency (IAF, (36)): slow frequency band from 1 Hz to 7 Hz (delta-theta), from IAF – 2 Hz to IAF (low alpha), from IAF to IAF + 2 Hz (high alpha), from 13 Hz to 25 Hz (beta). Band power values were log-transformed.

For microstate analysis, the procedure detailed in Murray et al. (37) was followed. Briefly, the optimal number of templates was chosen for each subject by means of the Krzanowski-Lai criterion (23) and a two-step clustering procedure was applied to obtain microstate templates separately for the group of patients and healthy controls (38). Differences between the templates of the two groups were assessed by means of Topographical Analysis of Variance (TANOVA). Since no differences were found between the 2 groups, one set of "global" maps, representing the data of all subjects, was obtained by clustering the individual maps considering both patients and healthy controls. These global templates were fitted backward to the original data on the basis of the maximum spatial correlation between each template and the EEG topography at each time instant. Then, for each subject and for each microstate template, the following metrics were calculated (39): mean microstate duration (in milliseconds), mean occurrence per second and mean percentage of covered analysis time. Overall metrics (duration and occurrence) were also calculated as the average of the metrics of all microstate templates.

Statistical Analysis

The Wilcoxon signed-rank test was used to compare clinical scores in patients at T0 and T1.

Band power statistical analysis

Difference between patients and healthy controls of spectral band power was assessed by a nonparametric cluster-based permutation procedure (12000 permutations), applied by means of the FieldTrip toolbox (40,41). Spearman's correlations were performed between each EEG frequency band power of each electrode and ALSFRS-R score. To take into account multiple comparisons across electrodes, the nonparametric cluster-based permutation procedure was also applied to correlation coefficients separately for each band (40, 41). IAF between patients and healthy controls was compared by means of the Mann-Whitney U test

A further Spearman's correlation was performed between the mean values of the band power of the significant clusters and *Disease progression* scores and the global average MRC scores, obtained as average of MRC across upper and lower limbs. Finally, to evidence differences in band power associated with clinical signs of disease progression, patients were split in 2 groups according to the King's score values (<4, 7 patients, =4, 8 patients) and band powers were compared between the 2 groups by means of a Mann-Whitney U test. The same comparisons were done classifying the patients in 2 groups according to MiToS scores (=1, 7 patients, >=2, 8 patients). Moreover, to evidence differences due to UMN involvement, patients were split in 2 groups (prevalent damage of UMN or LMN, Table 1), not differing for age or clinical scores. Band powers were compared between the 2 groups by means of a Mann-Whitney U test.

Microstate statistical analysis

The differences of microstate metrics between patients and healthy controls were evaluated by means of the Mann-Whitney U test, both considering the overall metrics

and separately for each microstate. False Discovery Rate (FDR) correction (Benjamini–Hochberg procedure) was applied including all microstate metrics within the same family. Microstate metrics were also compared between the 2 patient groups with different King or MiToS scores or prevalent UMN or LMN damage. The Spearman's correlation across patients between overall microstate metrics and clinical scores (ALSFR-S, *Disease progression* and the global average MRC scores) were calculated and FDR was applied for multiple comparison correction. A percentile-based bootstrap, with 5000 replicate samples, was applied to assess the 95% confidence interval of Spearman's rho-values.

Spearman's correlation was also calculated between beta power and microstate metrics.

Results

Clinical picture

Patients showed clinical worsening at T1 with respect to T0, as indicated by lower scores of ALSFRS-R and MRC at T1 for each limb (Table 3). The patients did not present evident cognitive involvement (mean MOCA score 26).

INSERT TABLE 3 HERE

Band power

Neither spectral power nor IAF showed difference between ALS patients and controls. A cluster of channels covering the centro-frontal regions was found with a significant negative correlation between ALSFRS-R scores and beta band (p=0.018, Fig.1a and Fig.1b). This correlation indicates that the patients with the higher beta power are those with worse clinical status.

INSERT FIGURE 1 HERE

The beta band power of the cluster negatively correlated with the global MRC score values (rho=-0.606, p=0.017, Confidence limit: [-0.84,-0.15], Fig.1c), and positively correlated with *Disease Progression* scores (rho=0.582, p=0.029, Confidence limit: [0.02,0.95], Fig.1d). The latter correlation evidenced that patients with higher beta power were those with higher clinical worsening at T1 with respect to T0. Finally, the beta power was higher in the group with higher disease burden (King's score = 4) with respect to the group with lower disease burden (King's score < 4): median [minimum-maximum]: 3.33 [2.19-3.60] vs 2.31 [1.21-3.12], respectively; Z=-2.55, p=0.009. The same result was found classifying the patients according to MiToS scores. The comparison of beta power between the group with higher disease burden and healthy controls did not reach the significance (p=0.145), although the median value of the patients was higher than the value of healthy controls (2.63 [1.25-3.28]). The comparison between the least severe patients and healthy controls did not show differences or trends (p>0.200). No difference in band powers were found between patients with damage of prevalent LMN or UMN involvement.

Microstates

The optimal number of microstate templates was found to be equal to 4 for both patients (Fig.2a) and healthy controls (Fig.2b). The mean EEG variance across subjects explained by microstates was 83.6±2.3 % for patients and 84.8±4.4 % for healthy controls. TANOVA did not show difference between microstate topographies of patients and healthy controls. For this reason, microstate metrics were evaluated on global maps (Fig.2c).

INSERT FIGURE 2 HERE

Microstate duration was longer in patients than in controls (Table 4). When looking at the single microstates, we found a difference between patients and healthy controls for microstate A and B duration (Table 4). Microstate occurrences of microstates A, C and D were lower in patients than in controls (Table 4). No difference between patients and healthy controls was found for microstate coverage.

When looking at the correlation between overall microstate features and clinical scores, we found only a negative correlation between microstate duration and ALSFRS-R scores (Spearman's rho=-0.662, p=0.008, Confidence limit: [-0.82,-0.16]), indicating that an increase of duration was paired to a worse clinical status.

INSERT TABLE 4 HERE

No difference in microstate metrics were found between patients with predominant LMN and UMN damage. Moreover, no relationship between microstate metrics and King's or MiToS's scores were found.

Correlation between microstates and beta power

No correlations between beta power and microstate features (duration, occurrence) were found.

Discussion

The goal of this study was to investigate the potential role of EEG features in defining a marker of disability in patients with ALS. Compared to other imaging techniques, the EEG has the advantage of being a direct measure of the neuronal activity, and as such it is an expression of functionality rather than of structure (42). We

showed a correlation between beta-band in motor/frontal regions and clinical severity, as captured by ALSFRS-R and MRC, as well as with *Disease Progression*. Differently from our results, previous EEG studies (19,20) did not find a direct correlation between EEG band powers and clinical status. This result can be explained by the clinical severity of the patient cohorts. Indeed, since we aimed at selecting a marker of disability, in this preliminary study we included a group of patients with more severe clinical conditions and longer disease duration than those examined in the previous EEG studies. The mean score (± standard deviation) of the ALSFRS-R scores in our patients was 28.5±9.2, while in (19) it was 36.0±7.8 and in (20) was 37.5±6.5. Although not reaching significant difference, the median of beta power was lower in healthy controls than in ALS patients with higher disease burden (King score values equal to 4). Future studies with adequate sample size are needed to assess whether beta power is higher in patients with higher disease burden.

Beta band activity in the motor areas has been traditionally associated to the steady-state of motor system in the healthy adult (43). The beta band activity has been hypothesized to represent the signature of an active process, which is needed to maintain the actual motor or cognitive state by impeding the elaboration of new movements or cognitive processes (44). In this framework, beta band activity can be considered as a sort of 'inertia' of the system, which cancels the effects of potentially new or unexpected external events (44–48). In this context, we can interpret our result on the correlation of the beta power with the severity in ALS patients as a sort of up regulation of steady state motor system. In patients with greater disability, in which the power in the beta band is greater, we can hypothesize an inability of the motor system to fast changes. This aspect, found for the beta band in motor regions, can be extended to non-motor areas, looking at the microstate features.

A major advantage of microstate analysis, with respect to power or connectivity analysis, is that they estimate the global dynamics of widespread networks, with an informative framework on neural activity dynamics without any type of a priori hypothesis (e.g. electrode location or specific frequencies). Moreover, previous studies demonstrated that microstates can be estimated even with a low number of EEG channels, highlighting the potentiality of this kind of analysis in a clinical context. We found that microstate duration was longer in patients than in controls. Furthermore, the overall longer duration of the microstates is correlated with a worse clinical status. The mean duration of microstates has traditionally been interpreted to reflect the stability of brain dynamics (22). Thus, a higher microstate duration can be thought as a greater reluctance of the system to change state. Interestingly, the duration of the microstates correlates with the ALSFRS-R, but not with the MRC scores. It should be noted that the ALSFRS-R is a global functional index of disability, while the MRC is an index of muscle weakness and so of exclusively motor involvement. In accordance with previous findings (27,28,49), microstates have been associated with cognitive networks only. The possible impairment of both motor and non-motor network activities to fast modify their status can be interpreted as an attempt in ALS patients to compensate the disability but resulting in an ineffective and probably maladaptive behaviour. Finally, although future studies are needed to address this point, we can speculate on the role of the EEG as a possible marker of early cognitive-behavioral dysfunction in ALS patients who do not yet have cognitive alterations found on neuropsychological routine tests.

No correlation between the microstates and the beta band was found, highlighting that both are independently associated with greater disability and could explain different aspects of disease severity.

In conclusion, our results showed that beta-band power and microstate metrics may be good candidates of disease severity and involvement in both motor and non motor regions, in ALS. Given the small number of patients enrolled, our preliminary results must be replicated and validated on a larger cohort of ALS patients. Moreover, in patients we studied, beta band increase correlated also with faster disease progression. Nevertheless, this result should be confirmed in follow-up studies, considering clinical scores and EEG features at different times.

Acknowledgements

Authors thank professor Nicola Ticozzi, who critically reviewed the manuscript.

Disclosure Statement

The authors report there are no competing interests to declare.

Data Availability Statement

The data that support the findings of this study are available from the corresponding author, PC, upon reasonable request.

References

1. Brooks BR. El Escorial World Federation of Neurology criteria for the diagnosis of amyotrophic lateral sclerosis. Subcommittee on Motor Neuron Diseases/Amyotrophic Lateral Sclerosis of the World Federation of Neurology Research Group on Neuromuscular Diseases and the El Escorial "Clinical limits of amyotrophic lateral sclerosis" workshop contributors. J Neurol Sci. 1994;124 Suppl:96–107. doi: 10.1016/0022-510x(94)90191-0. Cited: in: : PMID: 7807156.

2. Brooks BR, Miller RG, Swash M, Munsat TL, World Federation of Neurology Research Group on Motor Neuron Diseases. El Escorial revisited: revised criteria for the diagnosis of amyotrophic lateral sclerosis. Amyotroph Lateral Scler Other Motor Neuron Disord. 2000;1:293–299. doi: 10.1080/146608200300079536. Cited: in: : PMID: 11464847.

3. Shefner JM, Al-Chalabi A, Baker MR, Cui L-Y, de Carvalho M, Eisen A, Grosskreutz J, Hardiman O, Henderson R, Matamala JM, et al. A proposal for new diagnostic criteria for ALS. Clin Neurophysiol. 2020;131:1975–1978. doi: 10.1016/j.clinph.2020.04.005. Cited: in: : PMID: 32387049.

4. Cedarbaum JM, Stambler N, Malta E, Fuller C, Hilt D, Thurmond B, Nakanishi A. The ALSFRS-R: a revised ALS functional rating scale that incorporates assessments of respiratory function. BDNF ALS Study Group (Phase III). J Neurol Sci. 1999;169:13–21. doi: 10.1016/s0022-510x(99)00210-5. Cited: in: : PMID: 10540002.

5. Verber NS, Shepheard SR, Sassani M, McDonough HE, Moore SA, Alix JJP, Wilkinson ID, Jenkins TM, Shaw PJ. Biomarkers in Motor Neuron Disease: A State of the Art Review. Front Neurol. 2019;10:291. doi: 10.3389/fneur.2019.00291. Cited: in: : PMID: 31001186.

6. Bryan WW, Reisch JS, McDonald G, Herbelin LL, Barohn RJ, Fleckenstein JL. Magnetic resonance imaging of muscle in amyotrophic lateral sclerosis. Neurology. 1998;51:110–113. doi: 10.1212/wnl.51.1.110. Cited: in: : PMID: 9674787.

7. Cha CH, Patten BM. Amyotrophic lateral sclerosis: abnormalities of the tongue on magnetic resonance imaging. Ann Neurol. 1989;25:468–472. doi: 10.1002/ana.410250508. Cited: in: : PMID: 2774487.

8. Simon NG, Lagopoulos J, Paling S, Pfluger C, Park SB, Howells J, Gallagher T, Kliot M, Henderson RD, Vucic S, et al. Peripheral nerve diffusion tensor imaging as a measure of disease progression in ALS. J Neurol. 2017;264:882–890. doi: 10.1007/s00415-017-8443-x. Cited: in: : PMID: 28265751.

9. de Albuquerque M, Branco LMT, Rezende TJR, de Andrade HMT, Nucci A, França MC. Longitudinal evaluation of cerebral and spinal cord damage in Amyotrophic Lateral Sclerosis. Neuroimage Clin. 2017;14:269–276. doi: 10.1016/j.nicl.2017.01.024. Cited: in: : PMID: 28203530.

10. Meier JM, van der Burgh HK, Nitert AD, Bede P, de Lange SC, Hardiman O, van den Berg LH, van den Heuvel MP. Connectome-Based Propagation Model in Amyotrophic Lateral Sclerosis. Ann Neurol. 2020;87:725–738. doi: 10.1002/ana.25706. Cited: in: : PMID: 32072667.

11. Agosta F, Canu E, Valsasina P, Riva N, Prelle A, Comi G, Filippi M. Divergent brain network connectivity in amyotrophic lateral sclerosis. Neurobiol Aging. 2013;34:419–427. doi: 10.1016/j.neurobiolaging.2012.04.015. Cited: in: : PMID: 22608240.

12. Li F, Zhou F, Huang M, Gong H, Xu R. Frequency-Specific Abnormalities of Intrinsic Functional Connectivity Strength among Patients with Amyotrophic Lateral Sclerosis: A Resting-State fMRI Study. Front Aging Neurosci. 2017;9:351. doi: 10.3389/fnagi.2017.00351. Cited: in: : PMID: 29163133.

13. Mohammadi B, Kollewe K, Samii A, Krampfl K, Dengler R, Münte TF. Changes of resting state brain networks in amyotrophic lateral sclerosis. Exp Neurol. 2009;217:147–153. doi: 10.1016/j.expneurol.2009.01.025. Cited: in: : PMID: 19416664.

14. Schulthess I, Gorges M, Müller H-P, Lulé D, Del Tredici K, Ludolph AC, Kassubek J. Functional connectivity changes resemble patterns of pTDP-43 pathology in amyotrophic lateral sclerosis. Sci Rep. 2016;6:38391. doi: 10.1038/srep38391. Cited: in: : PMID: 27929102.

15. Trojsi F, Di Nardo F, Siciliano M, Caiazzo G, Passaniti C, D'Alvano G, Ricciardi D, Russo A, Bisecco A, Lavorgna L, et al. Resting state functional MRI brain signatures of fast disease progression in amyotrophic lateral sclerosis: a retrospective study. Amyotroph Lateral Scler Frontotemporal Degener. 2021;22:117–126. doi: 10.1080/21678421.2020.1813306. Cited: in: : PMID: 32885698.

16. Blain-Moraes S, Mashour GA, Lee H, Huggins JE, Lee U. Altered cortical communication in amyotrophic lateral sclerosis. Neurosci Lett. 2013;543:172–176. doi: 10.1016/j.neulet.2013.03.028. Cited: in: : PMID: 23567743.

17. Iyer PM, Egan C, Pinto-Grau M, Burke T, Elamin M, Nasseroleslami B, Pender N, Lalor EC, Hardiman O. Functional Connectivity Changes in Resting-State EEG as Potential Biomarker for Amyotrophic Lateral Sclerosis. PLoS One. 2015;10:e0128682. doi: 10.1371/journal.pone.0128682. Cited: in: : PMID: 26091258.

18. Fraschini M, Demuru M, Hillebrand A, Cuccu L, Porcu S, Di Stefano F, Puligheddu M, Floris G, Borghero G, Marrosu F. EEG functional network topology is associated with disability in patients with amyotrophic lateral sclerosis. Sci Rep. 2016;6:38653. doi: 10.1038/srep38653. Cited: in: : PMID: 27924954.

19. Nasseroleslami B, Dukic S, Broderick M, Mohr K, Schuster C, Gavin B, McLaughlin R, Heverin M, Vajda A, Iyer PM, et al. Characteristic Increases in EEG Connectivity Correlate With Changes of Structural MRI in Amyotrophic

Lateral Sclerosis. Cereb Cortex. 2019;29:27–41. doi: 10.1093/cercor/bhx301. Cited: in: : PMID: 29136131.

20. Dukic S, McMackin R, Buxo T, Fasano A, Chipika R, Pinto-Grau M, Costello E, Schuster C, Hammond M, Heverin M, et al. Patterned functional network disruption in amyotrophic lateral sclerosis. Hum Brain Mapp. 2019;40:4827–4842. doi: 10.1002/hbm.24740. Cited: in: : PMID: 31348605.

21. van der Graaff MM, de Jong JMBV, Baas F, de Visser M. Upper motor neuron and extra-motor neuron involvement in amyotrophic lateral sclerosis: a clinical and brain imaging review. Neuromuscul Disord. 2009;19:53–58. doi: 10.1016/j.nmd.2008.10.002. Cited: in: : PMID: 19070491.

22. Custo A, Van De Ville D, Wells WM, Tomescu MI, Brunet D, Michel CM. Electroencephalographic Resting-State Networks: Source Localization of Microstates. Brain Connect. 2017;7:671–682. doi: 10.1089/brain.2016.0476. Cited: in: : PMID: 28938855.

23. Murray MM, Brunet D, Michel CM. Topographic ERP Analyses: A Step-by-Step Tutorial Review. Brain Topogr. 2008;20:249–264. doi: 10.1007/s10548-008-0054-5.

24. Britz J, Díaz Hernàndez L, Ro T, Michel CM. EEG-microstate dependent emergence of perceptual awareness. Front Behav Neurosci. 2014;8:163. doi: 10.3389/fnbeh.2014.00163. Cited: in: : PMID: 24860450.

25. Croce P, Zappasodi F, Capotosto P. Offline stimulation of human parietal cortex differently affects resting EEG microstates. Sci Rep. 2018;8:1287. doi: 10.1038/s41598-018-19698-z.

26. Croce P, Zappasodi F, Spadone S, Capotosto P. Magnetic stimulation selectively affects pre-stimulus EEG microstates. NeuroImage. 2018;176:239–245. doi: 10.1016/j.neuroimage.2018.04.061.

27. Milz P, Faber PL, Lehmann D, Koenig T, Kochi K, Pascual-Marqui RD. The functional significance of EEG microstates--Associations with modalities of thinking. Neuroimage. 2016;125:643–656. doi: 10.1016/j.neuroimage.2015.08.023. Cited: in: : PMID: 26285079.

28. Seitzman BA, Abell M, Bartley SC, Erickson MA, Bolbecker AR, Hetrick WP. Cognitive manipulation of brain electric microstates. Neuroimage. 2017;146:533–543. doi: 10.1016/j.neuroimage.2016.10.002. Cited: in: : PMID: 27742598.

29. da Cruz JR, Favrod O, Roinishvili M, Chkonia E, Brand A, Mohr C, Figueiredo P, Herzog MH. EEG microstates are a candidate endophenotype for schizophrenia. Nat Commun. 2020;11:3089. doi: 10.1038/s41467-020-16914-1. Cited: in: : PMID: 32555168.

30. Vellante F, Ferri F, Baroni G, Croce P, Migliorati D, Pettoruso M, De Berardis D, Martinotti G, Zappasodi F, Giannantonio MD. Euthymic bipolar disorder patients

and EEG microstates: a neural signature of their abnormal self experience? Journal of Affective Disorders. 2020;272:326–334. doi: 10.1016/j.jad.2020.03.175.

31. Zappasodi F, Croce P, Giordani A, Assenza G, Giannantoni NM, Profice P, Granata G, Rossini PM, Tecchio F. Prognostic Value of EEG Microstates in Acute Stroke. Brain Topogr. 2017;30:698–710. doi: 10.1007/s10548-017-0572-0.

32. Sikka A, Jamalabadi H, Krylova M, Alizadeh S, van der Meer JN, Danyeli L, Deliano M, Vicheva P, Hahn T, Koenig T, et al. Investigating the temporal dynamics of electroencephalogram (EEG) microstates using recurrent neural networks. Hum Brain Mapp. 2020;41:2334–2346. doi: 10.1002/hbm.24949. Cited: in: : PMID: 32090423.

33. Ferree TC. Spherical splines and average referencing in scalp electroencephalography. Brain Topogr. 2006;19:43–52. doi: 10.1007/s10548-006-0011-0. Cited: in: : PMID: 17019635.

34. Barbati G, Porcaro C, Zappasodi F, Rossini PM, Tecchio F. Optimization of an independent component analysis approach for artifact identification and removal in magnetoencephalographic signals. Clin Neurophysiol. 2004;115:1220–1232. doi: 10.1016/j.clinph.2003.12.015. Cited: in: : PMID: 15066548.

35. Croce P, Zappasodi F, Marzetti L, Merla A, Pizzella V, Chiarelli AM. Deep Convolutional Neural Networks for Feature-Less Automatic Classification of Independent Components in Multi-Channel Electrophysiological Brain Recordings. IEEE Trans Biomed Eng. 2019;66:2372–2380. doi: 10.1109/TBME.2018.2889512.

36. Klimesch W. EEG alpha and theta oscillations reflect cognitive and memory performance: a review and analysis. Brain Res Brain Res Rev. 1999;29:169–195. doi: 10.1016/s0165-0173(98)00056-3. Cited: in: : PMID: 10209231.

37. Michel CM, Koenig T. EEG microstates as a tool for studying the temporal dynamics of whole-brain neuronal networks: A review. Neuroimage. 2018;180:577–593. doi: 10.1016/j.neuroimage.2017.11.062. Cited: in: : PMID: 29196270.

38. Michel CM, Koenig T, Brandeis D, Gianotti LRR, Wackermann J, editors. Electrical Neuroimaging [Internet]. Cambridge: Cambridge University Press; 2009 [cited 2022 Sep 14]. Available from: https://www.cambridge.org/core/books/electrical-neuroimaging/DB6F5991EF51762172A59823E132905E.

39. Brunet D, Murray MM, Michel CM. Spatiotemporal analysis of multichannel EEG: CARTOOL. Comput Intell Neurosci. 2011;2011:813870. doi: 10.1155/2011/813870. Cited: in: : PMID: 21253358.

40. Maris E, Oostenveld R. Nonparametric statistical testing of EEG- and MEG-data. J Neurosci Methods. 2007;164:177–190. doi: 10.1016/j.jneumeth.2007.03.024. Cited: in: : PMID: 17517438.

41. Oostenveld R, Fries P, Maris E, Schoffelen J-M. FieldTrip: Open source software for advanced analysis of MEG, EEG, and invasive electrophysiological data. Comput Intell Neurosci. 2011;2011:156869. doi: 10.1155/2011/156869. Cited: in: : PMID: 21253357.

42. Müller-Putz GR. Electroencephalography. Handb Clin Neurol. 2020;168:249–262. doi: 10.1016/B978-0-444-63934-9.00018-4. Cited: in: : PMID: 32164856.

43. Del Campo-Vera RM, Gogia AS, Chen K-H, Sebastian R, Kramer DR, Lee MB, Peng T, Tafreshi A, Barbaro MF, Liu CY, et al. Beta-band power modulation in the human hippocampus during a reaching task. J Neural Eng. 2020;17:036022. doi: 10.1088/1741-2552/ab937f. Cited: in: : PMID: 32413878.

44. Engel AK, Fries P. Beta-band oscillations--signalling the status quo? Curr Opin Neurobiol. 2010;20:156–165. doi: 10.1016/j.conb.2010.02.015. Cited: in: : PMID: 20359884.

45. Androulidakis AG, Jones SJ. Detection of signals in modulated and unmodulated noise observed using auditory evoked potentials. Clin Neurophysiol. 2006;117:1783–1793. doi: 10.1016/j.clinph.2006.04.011. Cited: in: : PMID: 16793334.

46. Baker SN. Oscillatory interactions between sensorimotor cortex and the periphery. Curr Opin Neurobiol. 2007;17:649–655. doi: 10.1016/j.conb.2008.01.007. Cited: in: : PMID: 18339546.

47. Gilbertson T, Lalo E, Doyle L, Di Lazzaro V, Cioni B, Brown P. Existing motor state is favored at the expense of new movement during 13-35 Hz oscillatory synchrony in the human corticospinal system. J Neurosci. 2005;25:7771–7779. doi: 10.1523/JNEUROSCI.1762-05.2005. Cited: in: : PMID: 16120778.

48. Schoffelen J-M, Oostenveld R, Fries P. Neuronal coherence as a mechanism of effective corticospinal interaction. Science. 2005;308:111–113. doi: 10.1126/science.1107027. Cited: in: : PMID: 15802603.

49. Britz J, Van De Ville D, Michel CM. BOLD correlates of EEG topography reveal rapid resting-state network dynamics. Neuroimage. 2010;52:1162–1170. doi: 10.1016/j.neuroimage.2010.02.052. Cited: in: : PMID: 20188188.

Table 1. Patient and healthy control characteristic.

	ALS patients (n = 15)	Healthy controls (n = 15)
Mean Age (standard deviation)	67.9 ± 10.9 years	68.4 ± 8.0 years
Gender	12 M, 3 F	11 M, 4 F
Mean time delay (standard deviation) between diagnosis and EEG recording	24.3 ± 17.9 months	
Inclusion criteria	- ALS, probable ALS or ALS probable with support of laboratory data according to the revised El Escorial criteria	
Exclusion criteria	- co-presence of other central nervous system diseases - previous polio infection - motor neuron diseases other than ALS (progressive bulbar paralysis, progressive muscle atrophy, primary lateral sclerosis) - clinical involvement of other neurological systems (sensory, extrapyramidal, oculomotor, cerebellar, vegetative) - other causes of significant focal or diffuse brain damage to conventional MRI - serious pathologies affecting any organ or system	
Median symptom duration at recruitment [min-max]	27 months [12 – 64]	
Patients needed non-invasive assisted ventilation	8 Period: 13months (1 – 36 months)	
Patients with prevalent damage of LMN or UMN	9 LMN, 6 UMN	

Table 2. Tests for clinical and neuropsychological evaluation

Clinical/Neuropsycological Scale		Description
ALS Functional Rating Scale-Revised (4)	**ALSFRS-R**	Evaluation of disease. The scale has a range from 0 to 48 points (12 x 0-4, where 0 indicates a total loss of function).
Manual muscle testing score	**MRC score**	Definition of the entity and the diffusion of the muscle deficit. Acquired for each upper (deltoid, biceps, common extensor of the fingers, interosseous muscles of the fingers) and lower limb (iliopsoas, quadriceps femoris, tibialis anterior, gastrocnemius). The scale has a range from 0 (total loss of function) to 5 points.
Forced Vital Capacity	**FVC**	Spirometry
ALS Assessment Questionnaire (33) (in the validated Italian version)	**ALSAQ-5**	Assessment of subjective well-being of patients
King's score (34)	**King**	Clinical staging of disease progression. Five stages (from 1 to 5) are defined, based on disease burden as measured by clinical involvement and significant feeding or respiratory failure: stage 1 corresponds to symptom onset and stage 5 to death.
MiToS score (34)	**MiToS**	While the King's clinical staging system is able to differentiate early to mid-disease well, the MiToS staging is able to differentiate late stages in detail. However, King's staging is mostly focused on anatomical disease spread and significant involvement of respiratory muscles, whereas MiToS staging is aimed more towards the distinction of functional capabilities during the spread of the disease.
Disease progression	*Diseasae Progression*	$\frac{(\text{ALSFRS-R at T0}) - (\text{ALSFRS-R at T1})}{\text{ALSFRS-R at T0}}$ Since a decrement of score at T1 indicates a clinical and functional worsening, a positive value of *Disease Progression* score indicates a percentage of clinical worsening at T1 with respect to T0.
Montreal Cognitive Assessment test (35)	**MoCA**	Neuropsychological evaluation, including a series of tests of visual-spatial/executive functions, naming, attention (selective and sustained attention, serial calculation), language (repetition and fluency), abstraction, deferred recall, orientation, for a total score of 30.

Table 3. Clinical scores (median, [minimum-maximum]) and Z-values [p-values] of Wilcoxon signed-rank test between T0 and T1 values.

	T0	**T1**	**Z value [p]**
ALSFRS-R	31.0 [*24.8 – 34.0*]	27.5 *[22.8 – 32.0]*	-2.68 [0.007]
MRC right upper limb	4.10 [*2.08 – 4.80*]	4.00 [*1.68 – 4.70*]	-2.83 [0.005]
MRC left upper limb	4.00 [*2.30 – 4.93*]	3.60 [1.68 – 4.20]	-3.07 [0.002]
MRC right lower limb	4.40 [*3.60 – 5.00*]	4.40 [*2.30 – 4.85*]	-2.21 [0.027]
MRC left lower limb	4.45 [*3.75 – 5.00*]	4.45 [*2.23 – 4.85*]	-2.03 [0.042]
ALSAQ-5	14.0 [*10.5-18.5*]	15.0 [*12.5 – 19.5*]	-2.41 [0.016]
Disease Progression	7 % [0 % – 25 %]		
MiToS score	2 [1 – 4]		
King's score	[2 – 4]		

Table 4. Differences of microstate metrics between patients and healthy controls.

		Overall	**A**	**B**	**C**	**D**
DURATION [ms]	*ALS*	82 [72-114]	85 [68-116]	84 [65-124]	87 [70-126]	70 [61-97]
	HC	67 [53-107]	63 [55-99]	61 [50-89]	62 [56-178]	64 [45-100]
	Z-value	-2.32	-2.59	*-3.13*	-2.01	-1.51
	p-value	***0.019****	***0.008****	***0.001****	0.045	0.137
OCCURRENCE [micr/s]	*ALS*	6.7 [4.5-8.8]	6.5 [4.9-8.8]	6.6 [4.1-8.8]	7.5 [4.1-8.5]	4.8 [2.4-7.4]
	HC	9.7 [4.7-21.4]	9.3 [4.0-25.9]	8.6 [3.4-19.3]	10.0 [4.4-25.8]	10.5 [3.4-19.2]
	Z-value	-2.17	-2.30	-1.31	-2.39	-3.01
	p-value	0.029	***0.021****	0.200	***0.016****	**0.003***
COVERAGE [%]	*ALS*	-	25 [11-27]	21 [9-29]	31 [12-54]	22 [10-44]
	HC	-	27 [15-41]	25 [18-37]	31 [17-37]	18 [10-25]
	Z-value	-	-0.22	-2.26	-0.23	-1.35
	p-value		>0.2	0.024	>0.2	0.187

Median and 5-95 percentile of microstate metrics of patients (ALS) and healthy controls (HC) are displayed. The Z-value and uncorrected p-value of the Mann-Whitney U test are also shown. Asterisks indicate significant test after FDR correction.

Figure 1. a) Topography of Spearman's rho values of the correlations between beta band power values and ALSFRS-R score values. Stars indicate significant clusters in the non-parametric permutation test. b) The cluster mean values of beta power over ALSFRS-R scores are shown. The regression line with R-value is also displayed. c) Beta power over global MRC scores. d) Beta power over global *Disease Progression* scores.

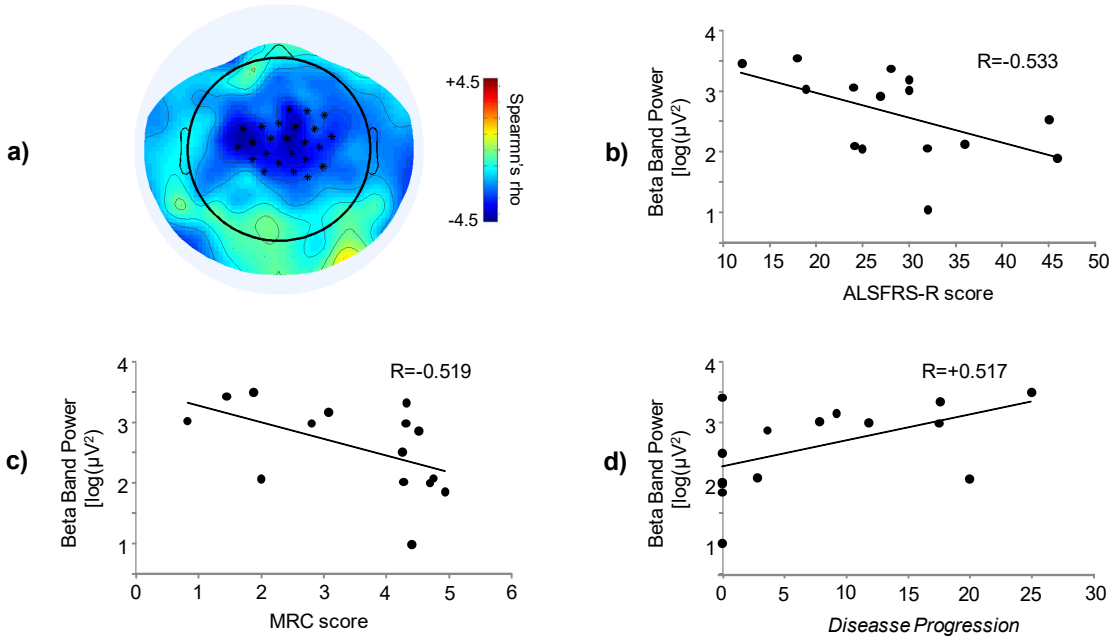

Figure 2. Topographic maps of the mean microstate templates as result of the clustering procedure applied to ALS patient group (a), healthy control group (b), the whole group of patients and controls (c). Red-blue colours indicate normalized positive-negative values. The microstate templates showed topographies similar to those obtained in previous studies: microstate A shows a left posterior to right frontal orientation; microstate B shows a right posterior to left frontal orientation; microstate C shows a symmetrical distribution between the two hemispheres, with an occipital to prefrontal orientation; microstate D shows a central activity.